Self-Assembly of Phosphate Fluorosurfactants in Carbon Dioxide

ARTICLE *in* LANGMUIR · MARCH 2004

Impact Factor: 4.46 · DOI: 10.1021/la034742s · Source: PubMed

Self-Assembly of Phosphate Fluorosurfactants in Carbon Dioxide

Jason S. Keiper,† Jacqueline A. Behles,† Tracy L. Bucholz,† Ruma Simhan,† and Joseph M. DeSimone*,†,‡

NSF Center for Environmentally Responsible Solvents and Processes, Department of Chemistry, University of North Carolina at Chapel Hill, Chapel Hill, North Carolina 27599, and Department of Chemical Engineering, North Carolina State University, Raleigh, North Carolina 27695

Gary W. Lynn, George D. Wignall,* and Yuri B. Melnichenko

Solid State Division, Oak Ridge National Laboratory,§ Oak Ridge, Tennessee 37831

Henrich Frielinghaus

Forschunszentrum Jülich GmbH, Institut für Festkörperforschung, D-52425 Jülich, Germany

Received May 1, 2003. In Final Form: December 1, 2003

Anionic phosphodiester surfactants, possessing either two fluorinated chains (**F/F**) or one hydrocarbon chain and one fluorinated chain (**H/F**), were synthesized and evaluated for solubility and self-assembly in liquid and supercritical carbon dioxide. Several surfactants, of both **F/F** and **H/F** types and having varied counterions, were found to be capable of solubilizing water-in-CO_2 (W/C), via the formation of microemulsions, expanding upon the family of phosphate fluorosurfactants already found to stabilize W/C microemulsions. Small-angle neutron scattering was used to directly characterize the microemulsion particles at varied temperatures, pressures, and water loadings, revealing behavior consistent with previous results on W/C microemulsions.

Introduction

Carbon dioxide (CO_2) is presently considered the most promising "green-friendly" alternative solvent.[1] Nonflammable, nontoxic, readily available, and inexpensive, CO_2 is a useful solvent in both its compressed liquid and supercritical ($scCO_2$; $T_{critical} = 31.1$ °C, $P_{critical} = 73.8$ bar) forms for a number of processes.[2] Although CO_2 solutions are prepared in pressurized vessels, with simple control of pressure and temperature, a wide range of solvent densities (and, in turn, solvent qualities and solvation properties) are attainable. Carbon dioxide is also easily recyclable and can be evaporated from reaction vessels through simple depressurization at ambient temperatures, allowing for low-energy, low-cost processing. Carbon dioxide is now used in extractions, cleaning systems, microelectronics development, and polymer production.[3]

An important hurdle to the use of CO_2 is the fact that many polar materials (such as water and ionic compounds) and high molecular weight polymers have low solubility in the medium[4] and are referred to as "CO_2-phobic".[5] To overcome this issue, surfactants must be employed to successfully disperse the normally incompatible solutes within CO_2. New applications and increased proliferation of CO_2 as a useful and versatile solvent in the chemical and biochemical realms depend to a great extent on the continued development of surface-active molecules capable of dispersing or solubilizing CO_2-phobic materials such as water. Fluorinated surfactants have served in this capacity for the stabilization of water-in-CO_2 via the formation of microemulsions.[6] Microemulsions are thermodynamically stable association colloids where a minor fluid phase is sequestered within a greater fluid phase, with surfactants adsorbed astride the two

* To whom correspondence should be addressed.

† NSF Center for Environmentally Responsible Solvents and Processes, Department of Chemistry, University of North Carolina at Chapel Hill.

‡ Department of Chemical Engineering, North Carolina State University Raleigh.

§ Managed by UT-Battelle, LLC, under Contract DE-AC05-00OR22725 with the U.S. Department of Energy

(1) DeSimone, J. M.; Keiper, J. S. *Curr. Opin. Solid State Mater. Sci.* **2001**, *5*, 333.

(2) Kendall, J. L.; Canelas, D. A.; Young, J. L.; DeSimone, J. M. *Chem. Rev.* **1999**, *99*, 543.

(3) Wells, S. L.; DeSimone, J. *Angew. Chem., Int. Ed.* **2001**, *40*, 518.

(4) Consani, K. A.; Smith, R. D. *J. Supercrit. Fluids* **1990**, *3*, 51.

(5) DeSimone, J. M.; Maury, E. E.; Menceloglu Y. Z.; McClain, J. B.; Romack, T. J.; Combes, J. R. *Science* **1994**, *265*, 365.

(6) Harrison, K.; Goveas, J.; Johnston, K. P.; O'Rear, E. A. *Langmuir* **1994,** *10*, 3536. (b) Johnston, K. P.; Harrison, K. L.; Clarke, M. J.; Howdle, S. M.; Heitz, M. P.; Bright, F. V.; Carlier, C.; Randolph, T. W. *Science* **1996**, *271*, 624. (c) Eastoe, J.; Bayazit, Z.; Martel, S.; Steytler, D. C.; Heenan, R. K. *Langmuir* **1996**, *12*, 1423. (d) Eastoe, J.; Cazelles, B. M. H.; Steytler, D. C.; Holmes, J. H.; Pitt, A. R.; Wear, T. J.; Heenan, R. K. *Langmuir* **1997**, *13*, 6980. (e) Zielinski, R. G.; Kline, S. R.; Kaler, E. W.; Rosov, N. *Langmuir* **1997**, *13*, 3934. (f) Holmes, J. D.; Bhargava, P. A.; Korgel, B. A.; Johnston, K. P. *Langmuir* **1999**, *15*, 6613. (g) Ji, M.; Chen, X.; Wai, C. M.; Fulton, J. L. *J. Am. Chem. Soc.* **1999,** *121*, 2631. (h) Jacobson, G. B.; Lee, C. T., Jr.; Johnston, K. P. *J. Org. Chem.* **1999**, *64*, 1201. (i) Eastoe, J.; Downer, A.; Paul, A.; Steytler, D. C.; Rumsey, E.; Penfold, J.; Heenan, R. K. *Phys. Chem. Chem. Phys.* **2000**, *2*, 5235. (j) Lee, C. T., Jr.; Bhargava, P.; Johnston, K. P. *J. Phys. Chem. B* **2000**, *104*, 4448. (k) Lee, C. T., Jr.; Johnston, K. P.; Dai, H. J.; Cochran, H. D.; Melnichenko, Y. B.; Wignall, G. D. *J. Phys. Chem. B* **2001**, *105*, 3540. (l) Liu, Z.-T.; Erkey, C. *Langmuir* **2001**, *17*, 274. (m) Ohde, H.; Hunt, F.; Kihura, S.; Wai, C. M. *Anal. Chem.* **2000**, *72*, 4738. (n) Lee, D.; Hutchison, J. C.; DeSimone, J. M.; Murray, R. M. *J. Am. Chem. Soc.* **2001**, *123*, 8406, (n) Lee, C. T., Jr.; Psathas, P. A.; Ziegler, K. J.; Johnston, K. P.; Dai, H. J.; Cochran, H. D.; Melnichenko, Y. B.; Wignall, G. D. *J. Phys. Chem. B* **2000**, *104*, 11094.

10.1021/la034742s CCC: $27.50
Published on Web 01/16/2004

Scheme 1. Synthesis of Phosphate Surfactants

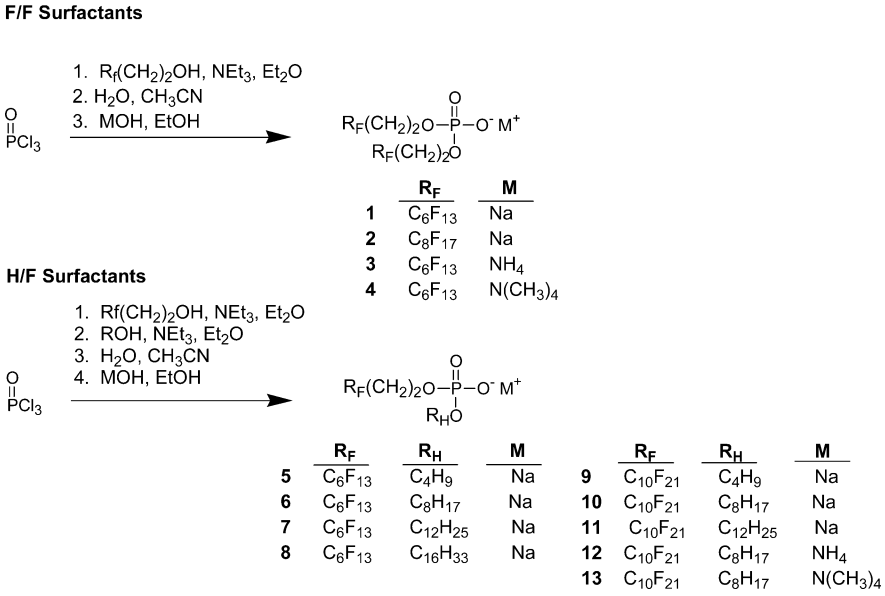

phases (often water and a hydrophobic solvent).[7] The surfactants serve to reduce the interfacial tension, and in order to carry out this task, the molecules must effectively pack about a curved surface while distributing appropriately between the phases of different polarities. Thus, both molecular geometry and makeup of the amphiphilic moieties play important roles. Only a few surfactant types have been used to form water-in-CO_2 (W/C) microemulsions, most commonly perfluoropolyether carboxylates and dichained sulfonate fluorosurfactants. Fluorinated surfactants are particularly suitable for W/C microemulsions due to the "CO_2-philicity"[8] of the fluorinated chains.

Phosphate esters are an important family of surfactants that have many industrial applications. There are a handful of examples of the use of phosphate fluorosurfactants in CO_2. Consani and Smith first reported that phosphate fluorosurfactants, in the form of a commercially available mixture, were capable of solubilizing small amounts of water in CO_2.[4] Interestingly, the surfactant *required* water to dissolve in CO_2. Wai and co-workers have used a phosphate acid-derivatized perfluoropolyether as a cosurfactant with Aerosol-OT (AOT) to stabilize W/C microemulsions.[6g,m] This surfactant system allowed for voltammetric studies and inorganic particle synthesis but was incapable of forming microemulsions as the sole surfactant. Recently, however, individual phosphate fluorosurfactants have been shown to form W/C microemulsions. Our groups,[9] as well as that of Eastoe et al.,[10] reported anionic phosphates capable of W/C microemulsion formation. In both studies, the surfactants allowed for considerable water content in the microemulsions (commonly described in terms of [water]/[surfactant] molar ratio, or W_o), and are thus promising materials for extending W/C microemulsions to a variety of applications.

In the present work we expand upon our initial report[9] on the behavior of anionic phosphate fluorosurfactants in carbon dioxide. The surfactants either possess two fluorinated chains (**F/F**) or one fluorinated and one fully hydrocarbon chain (**H/F**). The **H/F** surfactants, in particular, were inspired by hybrid sulfate surfactants that were shown to stabilize W/C microemulsions. Aspects of the surfactant structures that render them promising candidates for microemulsion formation include the following: (1) A very hydrophilic headgroup region capable of strongly structuring surrounding water molecules,[11] (2) CO_2-philic fluorinated chains, and (3) Nominal "inverted cone" geometry that lends toward packing in negative curvatures.[12]

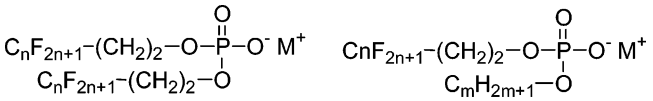

The surfactants were synthesized and evaluated for solubilities in CO_2 both in the absence and in presence of water via cloud point studies. It will be shown that several of the surfactants were capable of water uptake in CO_2, to different extents, and that the **F/F** and **H/F** surfactants display very different behavior. Small angle neutron scattering (SANS) was used to directly confirm the formation of nanometer-sized microemulsions and to quantify temperature- and pressure-induced changes in the size of their nanodroplet cores. Prospective future studies and potential applications will be discussed.

Results and Discussion

Synthesis. The present surfactants were prepared following the general procedures shown in Scheme 1. Protocols for **F/F** and **H/F** surfactant types involved reaction of stoichiometric amounts of long-chain alcohols with phosphorus oxychloride in the presence of triethylamine base, in anhydrous diethyl ether.[13] **H/F** surfactants synthesis required addition of the less reactive fluorinated

(7) *Handbook of Microemulsion Science and Technology*; Kumar, P., Mittal, K. L., Ed.; Marcel Dekker: New York, 1999.
(8) Maury, E. E.; Batten, H. J.; Killian, S. K.; Menceloglu, Y. Z.; Combes, J. R.; DeSimone, J. M. *Polym. Prepr.* **1993**, *34*, 664.
(9) Keiper, J. S.; Simhan, R.; DeSimone, J. M.; Wignall, G. D.; Melnichenko, Y. B.; Frielinghaus, H. *J. Am. Chem. Soc.* **2002**, *124*, 1834.
(10) Steytler, D. C.; Rumsey, E.; Thorpe, M.; Eastoe, J.; Paul, A.; Heenan, R. K. *Langmuir* **2001**, *17*, 7948.
(11) Tamaki, K. et al. *Bull. Chem. Soc. Jpn.* **1987**, *60*, 1225.
(12) Israelachvili, J. N. *Intermolecular and Surface Forces*, 2nd ed.; Academic Press: New York, 1999.
(13) Krafft, M.-P.; Rolland, J.-P.; Vierling, P.; Riess, J. G. *New. J. Chem.* **1990**, *14*, 869.

alcohol first, followed by the hydrocarbon alcohol. Upon hydrolysis in acetonitrile, the neutral compounds were obtained in unoptimized yields in the range of 30−60% and converted to their sodium salts with an equivalent of aqueous sodium hydroxide in ethanol.[14] Ammonium and tetramethylammonium salts were obtained by reaction with an equivalent of aqueous ammonium hydroxide and aqueous tetramethylammonium hydroxide in ethanol, respectively. Surfactant purity was determined by ^{1}H, ^{19}F, and ^{31}P NMR and elemental analysis.

Solubility and Phase Behavior. Phase behavior in CO_2 is commonly evaluated by determining so-called "cloud points" as a function of temperature and pressure. In brief, a typical experiment entails first dissolving the solute(s) in CO_2 within the confines of a stainless steel, variable volume view cell. By varying the volume with an adjustable piston, one can reduce the pressure isothermally, allowing the solution to pass through a pressure transition from clarity to phase separation. The transition is reversible upon repressurization. A cloud point is a somewhat subjective phenomenon as it is visually assessed, and there are intermediate changes in solution appearance that can occur. For instance, the solution can take on a deep orange color, presumably due to significant light scattering of agglomerating particles at pressures just above the cloud point.[3j] In the present study, cloud points were defined as the reproducible onset of a fully opaque solution and were taken on the cooling cycle over a range of temperatures. From these points, phase diagrams can be derived, defining the boundaries of solution stabilities.

Water uptake was evaluated for 2.5 wt % solutions of surfactants in CO_2 at varied W_o values.[15] **F/F** surfactants **1** and **2**, insoluble in dry CO_2, formed clear solutions in the presence of water. This behavior is consistent with Consani and Smith's previous findings with commercial anionic phosphate fluorosurfactants.[4] Figure 1 depicts cloud point measurements for surfactant **1** and **2** in graphs A and B, respectively. Two important items stand out in these results. First, both surfactants were capable of dissolving high loadings of water in CO_2, indicative of microemulsion formation. (The presence of discrete water pools for microemulsions of **1** was previously confirmed via solvatochromatic dye studies.[9]) Second, while surfactant **1** solutions provided linear cloud point trends over the studied temperature range, solutions of surfactant **2** either phase separated or had cloud point profiles that trended upward at temperatures below 35 °C. This surfactant pair is another instance where elongated CO_2-philic chains (surfactant **2** has longer fluorinated units than surfactant **1**) do not contribute to enhanced microemulsion stability. Erkey et al. observed similar results for sulfosuccinate fluorosurfactants.[6l]

Water uptake was also evaluated for 2.5 wt % solutions of surfactants using ammonium-based counterions. As opposed to surfactants having sodium counterions, surfactants possessing ammonium or tetramethylammonium counterions were soluble in dry CO_2 and formed clear solutions (data not shown).

In Figure 2, higher values of water uptake are examined for surfactants **1**, **3**, and **4**. Graphs A and B depict the cloud point profiles at $W_o = 34$ and 45, respectively. In graph A, surfactants **1** and **3** had similar profiles while surfactant **4** showed much different behavior. Surfactant

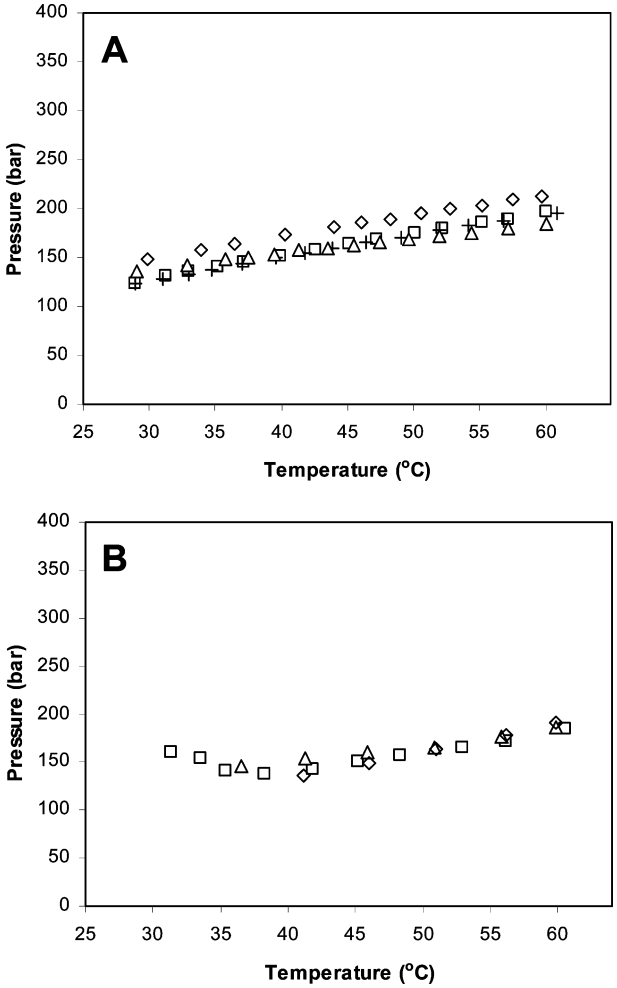

Figure 1. Cloud points of 2.5 wt % solutions of **F/F** anionic fluorosurfactants with various water loadings (uncorrected W_o) and sodium counterions: graph A, surfactant **1**, $W_o = 11$ (△), $W_o = 17$ (+), $W_o = 36$ (□), $W_o = 45$ (◇); graph B, surfactant **2,** $W_o = 11$ (△), $W_o = 33$ (□), $W_o = 46$ (◇).

4 also showed varying behavior in graph **B** as compared to surfactant **1**, while surfactant **3** was not able to form microemulsions at this water loading. Again, the behavior of surfactant **4** may indicate a change in the type of micelle formed in solution, such as from a more spherical micelle to a worm or threadlike micelle.

H/F surfactants were also evaluated for cloud point behavior at 2.5 wt %. Surfactants **5** through **8**, with $-(CH_2)_2C_6F_{13}$ fluorinated chains, were incapable of forming homogeneous solutions in the presence of water. Analogues **9** through **11**, with longer fluorinated $-(CH_2)_2C_{10}F_{21}$ units, were capable of water uptake, to varying degrees. Figure 3 depicts the cloud point profile for surfactant **10** (for comparison, please see the Supporting Information for the cloud point curves for surfactants **9** and **11**). In general, as the hydrocarbon chain length was increased, more water uptake was possible. (Below we report SANS measurements for surfactant **10** that provide evidence for the formation of discrete droplets.) Another possible factor is for surfactants **10** and **11**, higher loadings simply facilitated surfactant dissolution, or perhaps looser surfactant packing about the water phase, thus allowing for less unfavorable contact between the hydrocarbon and fluorinated chains. As with all surfactant solutions, however, a true explanation for the observed behavior likely lies in a complex balance of numerous competing and cooperative forces.

(14) Romsted, L. S.; Zanette, D. *J. Phys. Chem.* **1988**, *92*, 4690.

(15) For cloud point data and discussion of "dry" CO_2 solutions of the anionic surfactants and their neutral hydrogen phosphate precursors, please see the Supporting Information. Others have demonstrated the potential for micellization of surfactants in CO_2 in the absence of water.[16]

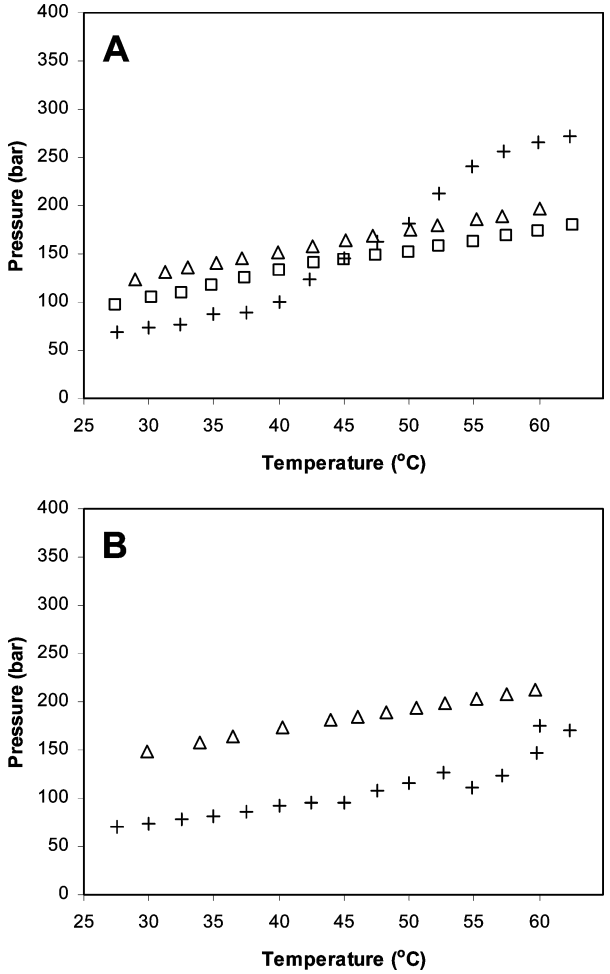

Figure 2. Cloud points of 2.5 wt % solutions of **F/F** anionic fluorosurfactants at constant W_o (uncorrected W_o) with varying counterions: surfactant **1** (△); surfactant **3** (□); surfactant **4** (+); graph A, $W_o = 34$; graph B, $W_o = 45$.

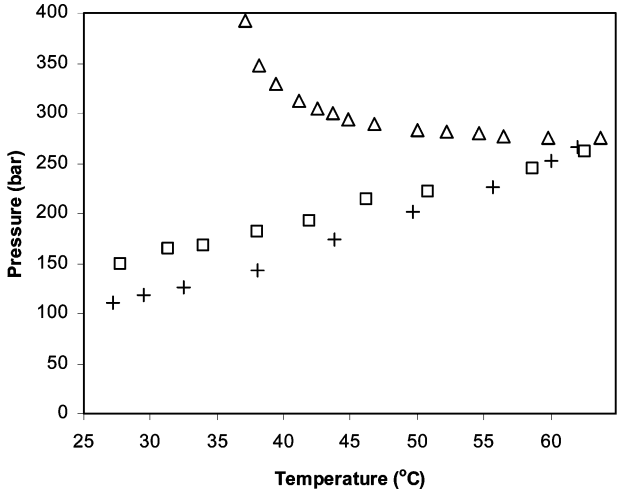

Figure 3. Cloud points of 2.5 wt % solution of **H/F** anionic fluorosurfactant **10** with various water loadings (uncorrected W_o): $W_o = 11$ (△); $W_o = 17$ (+); $W_o = 34$ (□).

Finally, in Figure 4, the influence of the counterion is examined for **H/F** surfactants, and the cloud point profiles for surfactants **10, 12**, and **13** are shown at $W_o = 11$. In each of the water loadings, the behavior of surfactant **12** did not show any sharp increases or decreases in solubility. Surfactants **10** and **13**, however, were shown to exhibit similar behavior, with surfactant **13** being the more readily

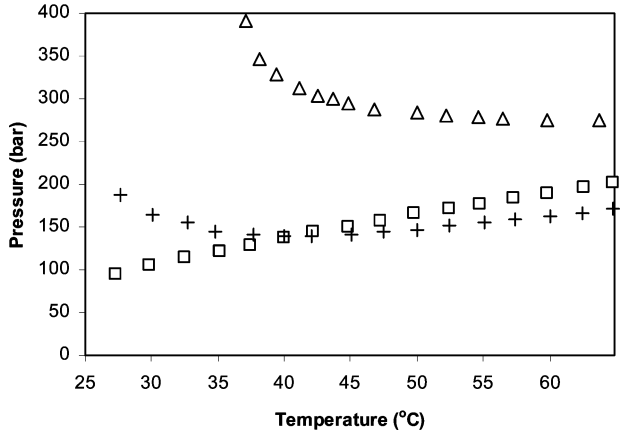

Figure 4. Cloud points of 2.5 wt % solutions of **H/F** anionic fluorosurfactants at constant $W_o = 11$ (uncorrected W_o): surfactant **10**, (△); surfactant **12**, (□); surfactant **13**, (+).

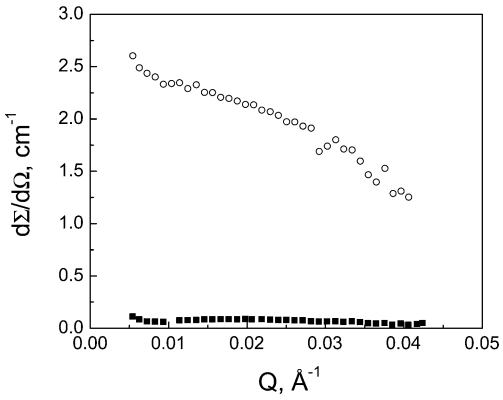

Figure 5. SANS cross sections for surfactant **1**: (■) 5.8 wt % swollen with D_2O ($W_o = 12.3$, uncorrected) and (○) 5.7 wt % swollen with H_2O ($W_o = 12.5$, uncorrected).

soluble of the two. With an increase in water loading, the solubility of the surfactants changed markedly (as shown in Figure 5 of Supporting Information at $W_o = 17$). Overall, this is the first report where the effect of the counterion on the surfactant was systematically studied for its corresponding effect on the phase behavior in CO_2. The effects of the changes in phase behavior seen with varying counterions may be explained by the counterion being able to affect the stability of the structure in solution based on its relative hydrophilicity as well as the strength of its binding to the headgroup of the surfactant.

Small-Angle Neutron Scattering (SANS). SANS measurements were carried out on the KWS2 SANS facility[17] at the FRJ2 reactor in Jülich, Germany, with a 45×45 cm^2 area detector with cell size ca. 0.8×0.8 cm^2 and a wavelength (λ) of 6 Å, with a wavelength polydispersity (Δ) $\lambda/\lambda = 0.2$. A sample−detector distance of 8 m was used to give an overall range of momentum transfer $0.0054 < Q = 4\pi\lambda^{-1} \sin\theta < 0.042$ Å^{-1}, where 2θ is the angle of scatter. The experiments were conducted in a cell that has been used extensively for previous neutron scattering experiments (23.1 mm path length, 5.6 cm^3 volume)[18,19] and due to the high penetrating power of

(16) Eastoe, J.; Paul, A.; Nave, S.; Steytler, D. C.; Robinson, B. H.; Rumsey, E.; Thorpe, M.; Heenan, R. K. *J. Am. Chem. Soc.* **2001**, *123*, 988.

(17) Neutronenstreuexperimente am FRJ2 in Jülich, 1997 (English and German texts are available from the Forschungszentrum Jülich, Germany).

(18) McClain, J.; Londono, J. D.; Chillura-Martino, D.; Triolo, R.; Betts, D. E.; Canelas, D. A.; Cochran, H. D.; Samulski, E. T.; DeSimone, J. M.; Wignall, G. D. *Science* **1996** *274*, 2049.

neutrons, the beam passed through two ~1 cm. thick sapphire windows with virtually no parasitic scattering or attenuation (cell transmission ~93%). All data sets were corrected for instrumental backgrounds[18,19] and normalized to an absolute (±4%) differential cross section per unit sample volume ($d\Sigma/d\Omega(Q)$ in units of cm^{-1}) by means of precalibrated secondary standards.[20] Depending on temperature and solvent density, small amounts of water dissolve in CO_2 (up to about 0.2 wt %). As with previous work in the literature,[6i] all W_o values reported here are based upon the amounts of surfactant and water added to the cell for each experiment and are uncorrected for this small effect.

The data were therefore analyzed as described previously[18,19] and the solutions were represented as a collection of polydisperse particles, assuming no orientational correlations, and the coherent differential scattering cross section is given by eq 1

$$\frac{d\Sigma}{d\Omega}(Q) = N_p[\langle|F(Q)|^2\rangle + |\langle F(Q)\rangle|^2 (S(Q) - 1)] + B \quad (1)$$

where N_p is the number density of particles, $S(Q)$ is the structure function arising from interparticle scattering, and B is the background from CO_2 (~0.04 cm^{-1}). Spherical particles with a centrosymmetric distribution of scattering length density may be modeled by concentric shells,[18,19] and for a core/shell micelle the intraparticle term in eq 1 may be expressed as

$$\langle|F(Q)|^2\rangle = \int |F(Q,R_1)|^2 f(R_1)\, dR_1 \quad (2)$$

where R_1 is the radius of a core, which occurs within the distribution of core radii with a normalized frequency of $f(R_1)$. The form factor of a particle with core radius R_1 and outer radius R_2 is given by

$$F(Q,R) = (4\pi/3)\,[R_1^3(\rho_1 - \rho_2)\,F_0(QR_1) + R_2^3(\rho_2 - \rho_s)\,F_0(QR_2)] \quad (3)$$

$$F_0(x) = \frac{3}{x^3}(\sin x - x\cos x)$$

Several particle shapes have been used to calculate the intraparticle term (or form factor) and in general for micelles in CO_2, the best fits have been given by a spherical core−shell model with a Schultz distribution[6i,10,18,19] of particle sizes

$$f(R_1) = \frac{(Z+1)^{Z+1}\, X^Z \exp[-(Z+1)X]}{\overline{R_1}\,\Gamma(Z+1)} \quad (4)$$

$$Z = \frac{1 - (\sigma/\overline{R_1})^2}{(\sigma/\overline{R_1})^2}$$

$$X = R_1/\overline{R_2}$$

where σ^2 is the variance of the distribution, Z is the breadth parameter, and ρ_1, ρ_2, and ρ_s are the scattering length densities (SLDs) of the core, shell, and solvent, respectively. As pointed out by Eastoe, Steytler, and co-workers,[6i] the SLD of D_2O (~6.4 × 10^{10} cm^{-2}) is much higher than the SLDs of CO_2 or the surfactants, both of which are ~2 × 10^{-2} cm^{-2}. Thus, the SLDs of the surfactant shell and CO_2 solvent are essentially matched ($\rho_2 \sim \rho_s$) and the scattering comes principally from the contrast between the D_2O core and CO_2. The particle form factor (defined as $P(Q)$ in ref 9), therefore reduces to a Bessel function representing a spherical core ($P(0) = 1$), and the water pools can be sized[6i] in terms of a core radius, R_1. This is illustrated in Figure 5 which shows the cross sections for solutions of 5.8 wt % surfactant **1** swollen with D_2O (W_o = 12.3) and 5.7 wt % surfactant **1** swollen with H_2O (W_o = 12.2), both at 173 bar after subtracting the CO_2 background. It may be seen that the cross section (~0.06 cm^{-1}) from the H_2O-swollen material is of the same order as the incoherent background and well over an order of magnitude less than the coherent cross section of the D_2O-swollen solution ($d\Sigma/d\Omega(0) \approx 3$ cm^{-1}). Thus, the majority of the scattering comes from the deuterium-labeled nanodroplets, which form the core of the microemulsions.

In our initial report,[9] particle interactions were neglected to a first approximation ($S(Q) \sim 1$) and $P(Q)$ was approximated[21] by $P(Q) \cong \exp[(-QR_g)^2/3]$, where R_g is the radius of gyration (i.e., the root mean square (rms) distance of all scattering elements from the center of gravity, $R_g^2 = \Sigma f_k r_k^2/\Sigma f_k$, and the summation runs over all scattering elements, k, thus, typical (Guinier) plots of $\ln[I(Q)]$ vs Q^2 are linear,[9] with slope $(R_g^2)/3$) and the corresponding core radii are given by $R_1 = (5/3)^{0.5}R_g$. In this paper, we extend the initial analysis and allow for polydispersity and also interparticle interactions between the droplets, which can cause $S(Q)$ to depart from unity in eq 1. Following the formalism employed by Steytler,[10] Eastoe,[6c,i] and Lee[6k,n] and co-workers, $S(Q)$ was modeled via an attractive Ornstein−Zernicke structure factor, characterized by a correlation length ξ and $S(0)$

$$S(Q) = 1 + \frac{S(0)}{(1 + Q^2\xi^2)} \quad (5)$$

Equation 5 has previously been applied[6i,c,10] to account for interactions for surfactant concentrations ~0.05 mol dm^{-3}, and in this work the vast majority of samples were in a similar concentration regime (<0.04 mol dm^{-3}), with the exception of a few samples discussed below. SANS data were therefore analyzed initially assuming that particle−particle interactions were negligible ($S(0) \approx 0$), as it has been previously observed[6i] that their effect is small for the values of W_o studied ($4 < W_o < 20$) in this concentration regime, and that in general, $S(Q)$ departed from unity only for high values ($W_o > 30$) of the water/surfactant ratio. Allowance for particle polydispersity was made via eq 4 and on average this reduced the core radius by typically ~20% from values derived from the Guinier formalism[21] used in the initial interpretation.[9] Allowing the Schultz breadth parameter to "float" generally resulted in values in the range $20 < Z < 30$ or $0.18 < \sigma/R_1 < 0.22$, and similar polydispersity parameters have been observed[6i,10] for other micelles formed by fluorosurfactants in CO_2. For a few systems with the highest values of W_o (19.4) and D_2O content (up to 4.4 vol %), $S(0)$ was also allowed to "float", along with the correlation length, ξ. The latter generally gave values typically 70−100 Å, and the analysis was found to be insensitive to ξ in this range, as previously observed.[6i] Fitting R_1, $S(0)$, and ξ, or fitting R_1, $S(0)$ with fixed $\xi \sim 100$ Å, generally gave values in the

(19) Triolo, F.; Triolo, A.; Triolo, R.; Londono, J. D.; Wignall, G. D.; McClain, J. B.; Betts, D. E.; Wells, S.; Samulski, E. T.; DeSimone, J. M. *Langmuir* **2000**, *16* (2), 416.

(20) Wignall, G. D.; Bates, F. S. *J. Appl. Crystallogr.* **1986**, *20*, 28.

(21) Guinier, A.; Fournet, G. *Small-Angle Scattering of X-rays*; Wiley: New York, 1955.

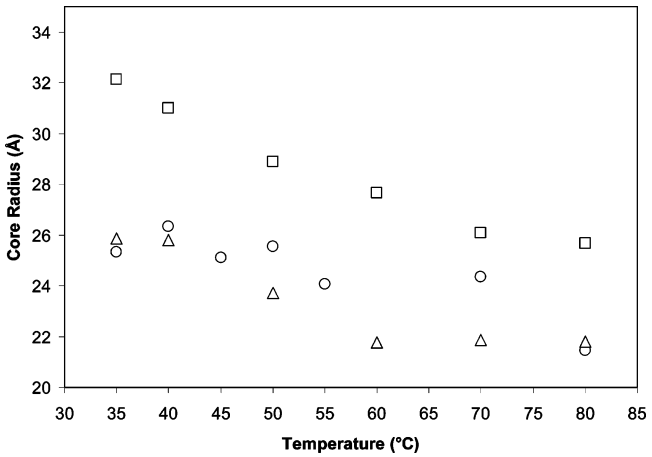

Figure 6. Surfactant **1**: R_1 vs T at 173 bar, for $W_o = 19.4$ (□), $W_o = 6.0$ (○), and $W_o = 3.9$ (△), all uncorrected.

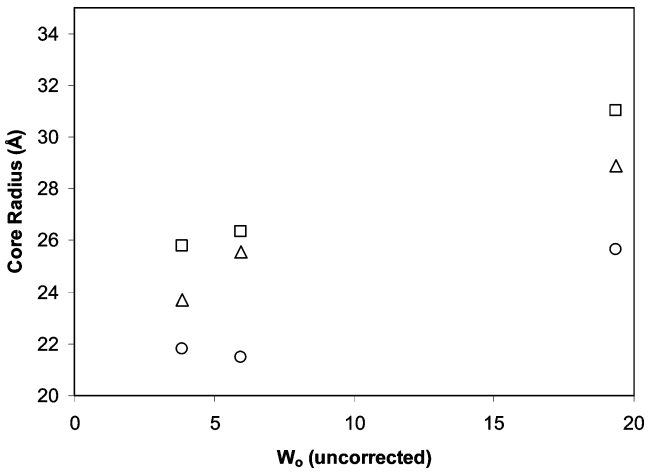

Figure 7. Surfactant **1**: R_1 vs uncorrected W_o at 173 bar at 40 °C (□), 50 °C (△), and 80 °C (○).

range $-0.1 < S(0) < 0.1$ confirming that the effect of interactions was small, even for the highest values of W_o and the volume fraction (4.5%) of D_2O, as expected from previous studies of similar systems.[6i,10] Thus, allowance for interactions, generally changed R_1 by less than 3%, which is less than the overall uncertainty in R_1 (±2 Å) generally expected from SANS analysis for similar systems.

The main conclusions emerging from the analysis are as follows: Figure 6 for surfactant **1** shows that for fixed initial pressure (172 psi) the core radius, R_1, falls 20−30% as the temperature is raised from 35 to 80 °C. This parallels the results of Eastoe et al. (see Figure 9 from ref 6i). Figure 7 shows that for fixed pressure, R_1 increases around 20% as W_o increases from 3.9 to 19.4, also paralleling the results of Eastoe et al. (see Figure 9 from ref 6i). Figure 8 shows that for fixed $W_o = 12.3$ (uncorrected) and temperature (24 °C), R_1 falls around 20% as the pressure increases from 173 to 380 bar, also consistent with the results of Eastoe et al. (see Figure 9 from ref 6i). Such behavior is consistent with a general increase in water solubility with increased CO_2 density, which would lead to "squeezing water out of the micelles" and rendering them smaller. It was found that for fixed pressure (414 bar), temperature (35 °C), and (initial) $W_o = 12.3$, the core radius increases with the volume % of D_2O (shown in Figure 6 of Supporting Information). This trend is reproduced for other pressures (e.g., 173, 310, and 414 bar) and temperatures (e.g., 24 °C) not shown. Finally, Figure 9 shows that at for fixed (initial) pressure, the core

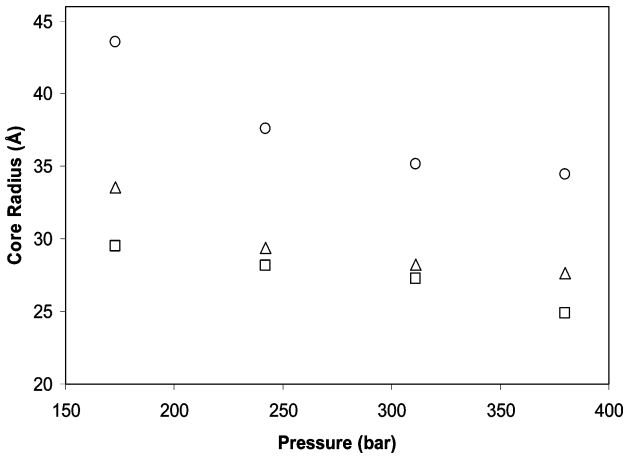

Figure 8. Surfactant **1**: R_1 vs P at 24 °C and $W_o = 12.3$ (uncorrected), and volume % D_2O = 4.4% (○), 1.5% (△), and 0.75% (□).

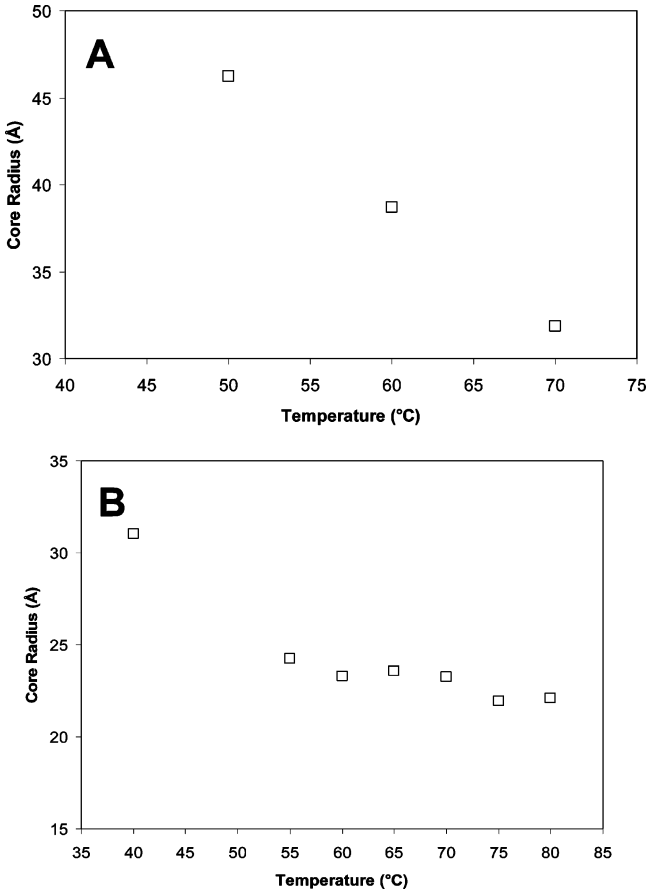

Figure 9. Graph A: surfactant **8**, R_1 vs T at 318 bar and $W_o = 12.6$ (uncorrected). Graph B: surfactant **2**, R_1 vs T at 242 bar and $W_o = 12.3$ (uncorrected).

radius, R_1, falls ~30% as the temperature is raised from 50 to 70 °C for surfactants **10** and **2**, respectively, again paralleling the results of Eastoe et al. (see Figure 9 in ref 6i).

It is important to emphasize that as progress continues on the fundamental development and characterization of new surfactants for CO_2, an eye should be kept toward applications that will spark continued interest in this emerging area of technology. In this regard, as a final note we report that several of the **H/F** surfactants, including surfactant **10**, formed bilayer vesicle structures in aqueous solution. Figure 10 depicts micrographs of

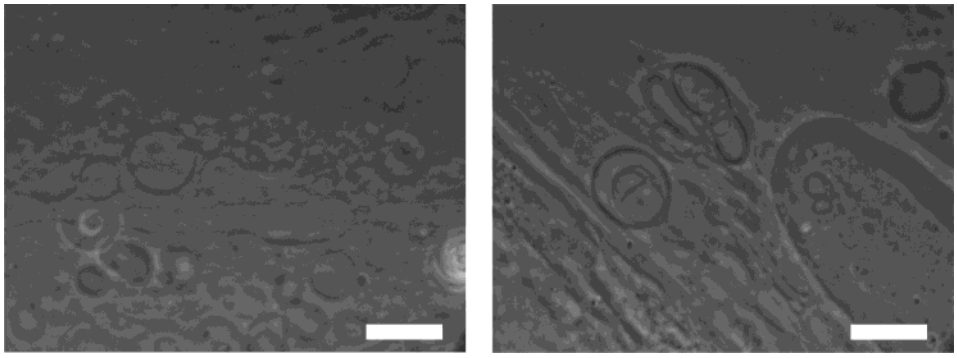

Figure 10. Microscopic bilayer vesicles of surfactant **10** in pure water at 25 °C. Bars = 30 μm.

micrometer-scale giant vesicles[22] that formed spontaneously when hydrated in pure water at room temperature. Vesicles (also known as liposomes) have been widely studied for drug delivery applications, and dense CO_2 has recently been reported as a processing solvent for vesicle formation through reverse phase evaporation.[23] Surfactant **10**, having both the capacity for stabilizing W/C microemulsions and forming vesicles in water, would seem to hold potential as a "dual" media surfactant capable of forming drug-encapsulating vesicles through W/C microemulsion intermediate assemblies.

Conclusions

Anionic phosphate fluorosurfactants have been shown to form W/C microemulsions, with the phase behavior dependent upon surfactant chain lengths, the nature of the chains (i.e., two fluorinated chains versus one fully hydrocarbon and one partially fluorinated chain), and the nature of the counterion (sodium, ammonium, and tetramethylammonium). SANS measurements on the microemulsions, modeled using the spherical core−shell model based upon a Schultz distribution, revealed particle radii trends (as a function of water loadings, pressure, and temperature) consistent with previous studies on similar W/C systems. Ongoing studies include molecular dynamics simulations,[24] NMR diffusion studies, and interfacial tension (IFT) measurements of the phosphate fluorosurfactants in CO_2. Future studies may probe the impact of different counterions, varied degrees of chain fluorination, and mixed surfactant systems on microemulsion behavior.

Experimental Section

Synthesis. Phosphorus oxychloride, triethylamine, 1-butanol, 1-octanol, 1-dodecanol, and 1-hexadecanol were purchased from Aldrich. Anhydrous diethyl ether was from Mallinckrodt, and acetonitrile from Fisher. The **F/F** and **H/F** surfactant series were synthesized as described above via procedures similar to those for surfactants **1** and **10**, respectively, as reported in the Supporting Information of ref 9. NMR analyses were carried out on either a 300 MHz Varian or 400 MHz Bruker apparatus. Elemental microanalyses were performed by Atlantic Microlab, Inc. (Norcross, GA).

Surfactant 1, Bis[2-(F-Hexyl)ethyl]phosphate, Sodium Salt (mp > 220 °C; 53% yield). ^{1}H NMR (300 MHz, δ, CD_3OD): 4.13 (q, 4H; J_{HH} = 6.6 Hz, J_{HP} = 6.8 Hz; CH_2O), 2.55 (tt, 4H; J_{HH} = 6.6 Hz, J_{HF} = 19.2 Hz; CF_2CH_2). ^{19}F NMR (282 MHz, δ, CD_3OD): −83.0 (CF_2CF_3), −115.1 (CH_2CF_2), −123.2, −124.2, −125.0 (3 × CF_2), −127.7 (CF_2CF_3). ^{31}P NMR (121 MHz, δ, CD_3OD): −0.65 ppm. Anal. Calcd: C, 23.66; H, 0.99. Found: C, 23.46; H, 1.00.

Surfactant 2, Bis[2-(F-Octyl)ethyl]phosphate, Sodium Salt (mp > 220 °C; 71% yield). ^{1}H NMR (300 MHz, δ, CD_3OD): 4.13 (q, 4H; J_{HH} = 6.3 Hz, J_{HP} = 7.3 Hz; CH_2O), 2.55 (tt, 4H; J_{HH} = 6.3 Hz, J_{HF} = 19.2 Hz; CF_2CH_2). ^{19}F NMR (282 MHz, δ,CD_3OD): −83.0 (CF_2CF_3), −114.9 (CH_2CF_2), −123.2, −123.3, −124.1, −125.0 (5 × CF_2), −127.7 (CF_2CF_3). ^{31}P NMR (121 MHz, δ, CD_3OD): 0.90 ppm. Anal. Calcd: C, 23.73; H, 0.80. Found: C, 23.44; H, 0.84.

Surfactant 3, Bis[2-(F-Hexyl)ethyl]phosphate, Ammonium Salt (mp = 200−205 °C; 42% yield). ^{1}H NMR (400 MHz, δ, CD_3OD): 4.14 (q, 4H; J_{HH} = 6.6 Hz, J_{HP} = 7.2 Hz; CH_2O), 2.55 (tt, 4H; J_{HH} = 6.8 Hz, J_{HF} = 19.2 Hz; CF_2CH_2). ^{19}F NMR (282 MHz, δ, CD_3OD): −82.9 (CF_2CF_3), −115.0 (CH_2CF_2), −123.4, −124.4, −125.2 (3 × CF_2), −127.8 (CF_2CF_3). ^{31}P NMR (121 MHz, δ, CD_3OD): 0.35 ppm. Anal. Calcd: C, 23.81; H, 1.50. Found: C, 23.83; H, 1.45.

Surfactant 4, Bis-[2-(F-Hexyl)ethyl]phosphate, Tetramethylammonium Salt (mp > 220 °C; 35% yield). ^{1}H NMR (400 MHz, δ, CD_3OD): 4.14 (q, 4H; J_{HH} = 6.4 Hz, J_{HP} = 6.8 Hz; CH_2O), 3.17 (s, 12H, $N(CH_3)_4$), 2.55 (tt, 4H; J_{HH} = 6.4 Hz, J_{HF} = 19.2 Hz; CF_2CH_2). ^{19}F NMR (282 MHz, δ, CD_3OD): −82.9 (CF_2CF_3), −115.0 (CH_2CF_2), −123.4, −124.4, −125.2 (3 × CF_2), −127.8 (CF_2CF_3). ^{31}P NMR (121 MHz, δ, CD_3OD): 0.35 ppm. Anal. Calcd: C, 27.83; H, 2.33. Found: C, 27.69; H, 2.46.

Surfactant 5, [2-(F-Hexyl)ethyl]butylphosphate, Sodium Salt (mp > 225 °C, 31% yield). ^{1}H NMR (400 MHz, δ, CD_3OD): 4.12 (q, 2H; J_{HH} = 6.8 Hz, J_{HP} = 7.5 Hz; R_F *chain* CH_2O), 3.83 (q, 2H; J_{HH} = 5.9 Hz, J_{HP} = 6.5 Hz; R_H *chain* CH_2O), 2.54 (tt, 2H; J_{HH} = 6.5 Hz, J_{HF} = 19.1 Hz; CF_2CH_2), 1.58 (m, 2H; $CH_2CH_2CH_2$O), 1.41 (m, 2H), 0.92 (t, 3H; J_{HH} = 7.0 Hz). ^{19}F NMR (282 MHz, δ, CD_3OD): −83.0 (CF_2CF_3), −114.9 (CH_2CF_2), −123.2, −124.2, −123.0, −127.6 (CF_2CF_3). ^{31}P NMR (121 MHz, δ, CD_3OD): 1.54. Anal. Calcd: C, 27.60; H, 2.51. Found: C, 27.35; H, 2.62.

Surfactant 6, [2-(F-Hexyl)ethyl]octylphosphate, Sodium Salt (mp > 225 °C, 57% yield). ^{1}H NMR (400 MHz, δ, CD_3OD): 4.15 (q, 2H; J_{HH} = 6.5 Hz, J_{HP} = 7.2 Hz; R_F *chain* CH_2O), 3.87 (q, 2H; J_{HH} = 6.0 Hz, J_{HP} = 6.4 Hz; R_H *chain* CH_2O) 2.59 (tt, 2H; J_{HH} = 6.6 Hz, J_{HF} = 19.1 Hz; CF_2CH_2), 1.6 (m, 2H; $CH_2CH_2CH_2$O), 1.25−1.43 (m, 10H), 0.91 t, 3H; J_{HH} = 7.0 Hz). ^{19}F NMR (of acid form) (282 MHz, δ, $CDCl_3$): −83.0 (CF_2CF_3), −114.9 (CH_2CF_2), −123.2, −124.2, −123.0, −127.6 (CF_2CF_3). ^{31}P NMR (of acid form) (121 MHz, δ, $CDCl_3$): 1.38.

Surfactant 7, [2-(F-Hexyl)ethyl]dodecylphosphate, Sodium Salt (mp > 225 °C, 62% yield). ^{1}H NMR (of acid form) (300 MHz, δ, $CDCl_3$): 4.1 (q, 2H; R_F *chain* CH_2O), 3.9 (q, 2H; R_H *chain* CH_2O), 2.5 (m, 2H; CF_2CH_2), 1.6 (m, 2H; $CH_2CH_2CH_2$O), 1.0−1.4 (m, 10H), 0.89 (t, 3H). ^{19}F NMR (of acid form) (282 MHz, δ, $CDCl_3$): −83.0 (CF_2CF_3), −114.9 (CH_2CF_2), −123.2, −124.2, −123.0, −127.6 (CF_2CF_3). ^{31}P NMR (of acid form) (121 MHz, δ, $CDCl_3$): 1.31.

Surfactant 8, [2-(F-Hexyl)ethyl]hexadecylphosphate, Sodium Salt (mp > 225 °C, 75% yield). ^{1}H NMR (400 MHz, δ, CD_3OD): 4.14 (q, 2H; J_{HH} = 6.8 Hz, J_{HP} = 7.2 Hz; R_F *chain* CH_2O),

(22) Menger, F. M.; Keiper, J. S. *Angew. Chem., Int. Ed. Engl.* **1998**, *37*, 3443.
(23) (a) Otake, K.; Imura, T.; Sakai, H.; Abe, M. *Langmuir* **2001**, *17*, 3898. (b) Imura, T.; Otake, K.; Hashimoto, S.; Gotoh, T.; Yuasa, M.; Yokoyama, S.; Sakai, H.; Rathman, J. F.; Abe, M. *Colloids Surf., B* **2003**, *27*, 133.
(24) Senapati, S.; Keiper, J. S.; Wignall, G. D.; Melnichenko, Y. B.; Frielinghaus, H.; DeSimone, J. M.; Berkowitz, M. L. *Langmuir* **2002**, *18*, 7371.

3.84 (q, 2H; J_{HH} = 6.4 Hz, J_{HP} = 6.4 Hz; R_H *chain* CH_2O) 2.56 (tt, 2H; J_{HH} = 6.6 Hz, J_{HF} = 18.8 Hz; CF_2CH_2), 1.61 (m, 2H; $CH_2CH_2CH_2O$), 1.28−1.38 (m, 26H), 0.89 (t, 3H; J_{HH} = 7.0 Hz). ^{19}F NMR (282 MHz, δ, $CDCl_3$): −85.0 (CF_2CF_3), −115 (CH_2CF_2), −120 (CF_2CF_3). ^{31}P NMR (121 MHz, δ, $CDCl_3$): 0.0. Anal. Calcd: C, 41.75; H, 5.40. Found: C, 42.03; H, 5.46.

Surfactant 9, [2-(F-Decyl)ethyl]butylphosphate, Sodium Salt (mp > 220 °C, 39% yield). ^{1}H NMR (400 MHz, δ, CD_3OD): 4.13 (q, 2H; J_{HH} = 6.5 Hz, J_{HP} = 7.6 Hz; R_F *chain* CH_2O), 3.83 (q, 2H; J_{HH} = 6.0 Hz, J_{HP} = 6.6 Hz; R_H *chain* CH_2O), 2.55 (tt, 2H; J_{HH} = 6.7 Hz, J_{HF} = 19.1 Hz; CF_2CH_2), 1.59 (m, 2H; CH_2CH_2-CH_2O), 1.40 (m, 2H), 0.92 (t, 3H; J_{HH} = 7.0 Hz). ^{19}F NMR (282 MHz, δ, CD_3OD): −83.0 (CF_2CF_3), −114.9 (CH_2CF_2), −123.0, −124.0, −125.0 (7 × CF_2), −127.6 (CF_2CF_3). ^{31}P NMR (121 MHz: δ, CD_3OD): 1.53. Anal. Calcd: C, 26.61; H, 1.81. Found: C, 26.45; H, 1.63.

Surfactant 10, [2-(F-Decyl)ethyl]octylphosphate, Sodium Salt (mp > 225 °C, 48% yield). ^{1}H NMR (400 MHz, δ, CD_3OD): 4.13 (q, 2H; J_{HH} = 6.3 Hz, J_{HP} = 7.0 Hz; R_F *chain* CH_2O), 3.82 (q, 2H; J_{HH} = 6.5 Hz, J_{HP} = 6.6 Hz; R_H *chain* CH_2O), 2.55 (tt, 2H; J_{HH} = 6.5 Hz, J_{HF} = 19.6 Hz; CF_2CH_2), 1.60 (m, 2H; $CH_2CH_2CH_2O$), 1.30−1.40 (br m, 10H), 0.87 (t, 3H; J_{HH} = 7.1 Hz). ^{19}F NMR (282 MHz, δ, CD_3OD): −81.4 (CF_2CF_3), −113.3 (CH_2CF_2), −121.4, −122.4, −123.4, (7 × CF_2), −126.0 (CF_2CF_3). ^{31}P NMR (121 MHz, δ, CD_3OD): 1.53. Anal. Calcd: C, 30.86; H, 2.72. Found: C, 30.73; H, 2.62.

Surfactant 11, [2-(F-Decyl)ethyl]dodecylphosphate, Sodium Salt (mp > 220 °C, 30% yield). ^{1}H NMR (400 MHz, δ, CD_3OD): 4.43 (q, 2H; J_{HH} = 6.5 Hz, J_{HP} = 7.2 Hz; R_F *chain* CH_2O), 3.83 (q, 2H; J_{HH} = 5.9 Hz, J_{HP} = 6.5 Hz; R_H *chain* CH_2O), 2.56 (tt, 2H; J_{HH} = 6.5 Hz, J_{HF} = 19.1 Hz; CF_2CH_2), 1.60 (m, 2H; $CH_2CH_2CH_2O$), 1.27−1.40 (br m, 18H), 0.88 (t, 3H; J_{HH} = 7.1 Hz). **^{19}F NMR:** (282 MHz, δ, CD_3OD) −82.9 (CF_2CF_3), −114.9 (CH_2CF_2), −123.0, −124.0, −124.9, (7 × CF_2), −127.6 (CF_2CF_3). ^{31}P NMR (121 MHz, δ, CD_3OD): 1.54. Anal. Calcd: C, 34.55; H, 3.50. Found: C, 34.79; H, 3.39.

Surfactant 12, [2-(F-Decyl)ethyl]octylphosphate, Ammonium Salt (mp > 220 °C, 28% yield). ^{1}H NMR (400 MHz, δ, CD_3OD): 4.12 (q, 2H; J_{HH} = 6.8 Hz, J_{HP} = 7.2 Hz; R_F *chain* CH_2O), 3.83 (q, 2H; J_{HH} = 6.4 Hz, J_{HP} = 6.4 Hz; R_H *chain* CH_2O), 2.58 (tt, 2H; J_{HH} = 6.4 Hz, J_{HF} = 18.8 Hz; CF_2CH_2), 1.61 (m, 2H; $CH_2CH_2CH_2O$), 1.28−1.37 (br m, 10H), 0.87 (t, 3H; J_{HH} = 7.2 Hz). ^{19}F NMR (282 MHz, δ, CD_3OD): −82.8 (CF_2CF_3), −115.0 (CH_2CF_2), −123.1, −124.2, −125.1 (7 × CF_2), −127.7 (CF_2CF_3). ^{31}P NMR (121 MHz, δ, CD_3OD): 0.98 ppm. Anal. Calcd: C, 31.06; H, 3.26. Found: C, 31.11; H, 3.20.

Surfactant 13, [2-(F-Decyl)ethyl]octylphosphate, Tetramethylammonium Salt (mp > 220 °C, 32% yield). ^{1}H NMR (400 MHz, δ, CD_3OD): 4.12 (q, 2H; J_{HH} = 6.6 Hz, J_{HP} = 7.2 Hz; R_F *chain* CH_2O), 3.82 (q, 2H; J_{HH} = 6.4 Hz, J_{HP} = 1.6 Hz; R_H *chain* CH_2O), 2.55 (tt, 2H; J_{HH} = 6.4 Hz, J_{HF} = 18.9 Hz; CF_2CH_2), 1.60 (m, 2H; $CH_2CH_2CH_2O$), 1.20−1.40 (br m, 10H), 0.87 (t, 3H; J_{HH} = 6.8 Hz). ^{19}F NMR (282 MHz, δ, CD_3OD): −82.8 (CF_2CF_3), −115.0 (CH_2CF_2), −123.1, −124.2, −125.1 (7 × CF_2), −127.7 (CF_2CF_3). ^{31}P NMR (121 MHz: δ, CD_3OD): 0.96 ppm. Anal. Calcd: C, 34.75; H, 4.01. Found: C, 34.42; H, 4.47.

Cloud Point Measurements. Cloud point solubilities of surfactants and surfactants and water in carbon dioxide were carried out using a HIP variable volume pressure generator/view cell (maximum volume = 15 mL) containing a 0.5 in. thick sapphire window for viewing and a magnetic stir bar to agitate the solution. CO_2 (Air Products) was injected with the aid of an ISCO compression pump connected to the cell through high-pressure steel tubing. The cell was further attached to a Sensotec pressure transducer and an Omega thermocouple for pressure and temperature readouts, respectively. Measured amounts of surfactant and water were added at room temperature prior to pressurization with CO_2. Samples were heated (controlled to ±0.1 °C) in the cell through the use of variac-controlled heating tape. Cloud points (judged as the reproducible, reversible onset of a visually fully opaque solution) were taken on the cooling cycle by isothermally varying the pressure through volume changes facilitated by the hand-controlled piston. The cell was tipped at a downward angle to aid in the observation of any phase-separated liquids. The cell was cleaned thoroughly between experiments.

UV−vis.[9] UV−vis spectra were acquired using a Perkin-Elmer Lambda 40 spectrometer. Pressurized solutions were prepared in a 2.5 mL stainless steel cell, equpped with two 1 in. diameter × $^5/_8$ in. thick sapphire windows enclosing a 1 cm solution path length. Appropriate amounts of surfactant and water were placed into the cell chamber, along with a $^1/_4$ in. magnetic stir bar for agitation. A film of methyl orange (for a concentration of 5×10^{-5} M) was precast and dried on one of the sapphire windows by addition of a stock solution via syringe. The chamber was tightly sealed, and the cell was pressurized and stirred until a clear, one-phase solution was present.

Small-Angle Neutron Scattering (SANS). SANS measurements were carried out on the KWS2 SANS facility at the FRJ2 reactor in Jülich, Germany, as described in detail above. CO_2 (Air Liquide) was pressurized using an HIP stainless steel generator, with aid of readings from a Sensotec pressure transducer. The temperature of the stainless steel solution chamber (5.6 mL volume) was controlled with electric heating sleeves. Sample solutions were prepared by loading the surfactant, D_2O (Cambridge Isotopes), and a "flea" magnetic stir bar to agitate the materials after injection of CO_2.

Microscopy. Surfactant samples (∼1 mg) were smeared on a borosilicate glass microscope slide with a spatula, hydrated with ∼200 μL of Milli-Q deionized water, and covered with a thin glass coverslip. Samples were allowed to hydrate at room temperature for a few minutes and were subsequently evaluated using a Nikon Diaphot TMD (phase contrast mode) outfitted with an Optronics digital camera and Image Pro Plus software.

Acknowledgment. This work was supported by the Kenan Center for the Utilization of Carbon Dioxide in Manufacturing and the STC Program of the National Science Foundation under Agreement CHE-9876674. The research at Oak Ridge was supported by the Division of Materials Sciences, under Contract No. DE-AC05-00OR22725 with the Oak Ridge National Laboratory, managed by UT-Battelle, LLC. SANS experiments were carried out at the KWS-2 facility at Forschungszentrum Jülich. J.S.K., G.D.W., Y.B.M. and G.W.L. wish to thank Professor D. Richter for the hospitality and assistance provided by the staff of the FZJ. We also thank Professor F. Menger (Emory University) for use of the optical microscope.

Supporting Information Available: Data and discussion on waterless surfactant−CO_2 solutions, cloud point profiles, and core radius vs volume of D_2O. This material is available free of charge via the Internet at http://pubs.acs.org.

LA034742S